Kinetic and ESR studies on radical polymerization. ESR and kinetic evidences for the penultimate effect in the radical-initiated copolymerization of *N*-cyclohexylmaleimide and bis(2-ethylhexyl) itaconate in benzene

Tsuneyuki Sato, Shinji Kawasaki, Makiko Seno, Hitoshi Tanaka*

Department of Chemical Science and Technology, Faculty of Engineering, Tokushima University, Minamijosanjima 2-1, Tokushima 770, Japan

Kenji Kato

Oita Plant, Nippon Oil & Fats Company, Ltd., Nakanosu 2, Oita 870-01, Japan

(Received: October 8, 1992)

SUMMARY:

The copolymerization of *N*-cyclohexylmaleimide (**1**) (M_1) and bis(2-ethylhexyl) itaconate (**2**) (M_2) with dimethyl 2,2′-azoisobutyrate (**3**) as an initiator was carried out at 50 °C in benzene. Monomer reactivity ratios were estimated as $r_1 = 0{,}34$ and $r_2 = 0{,}38$. The copolymerization rate (R_p) and the molecular weight of the resulting copolymer increased with increasing concentration of **1** when the total concentration of comonomers was fixed at 1,00 mol · L^{-1}. R_p was proportional to $[3]^{0,5}$, indicating a usual bimolecular termination in the copolymerization. An electron spin resonance (ESR) spectrum of the propagating polymer radicals was observable in the actual copolymerization system at 50 °C. The spectrum of the copolymerization system is inexplicable in terms of any superposition of spectra observed in the corresponding homopolymerization systems, revealing that some penultimate monomeric unit causes a change in the ESR spectrum, that is, the structure of propagating polymer radical. The apparent rate constant of propagation (k_p) and termination (k_t) were estimated by ESR. The k_p values (1,5 – 50 L · mol^{-1} · s^{-1}) are fairly higher than those estimated on the basis of the terminal model, affording another piece of evidence for the penultimate effect. The k_t value ($1{,}8 - 5{,}4 \cdot 10^3$ L · mol^{-1} · s^{-1}) shows a behaviour similar to that of the intrinsic viscosity of the resulting copolymer on varying the monomer feed composition, which seems to reflect diffusion-control of termination reactions.

Introduction

Itaconic acid esters, 1,1-disubstituted monomers, and maleimide derivatives, 1,2-disubstituted monomers, are well known to be easily polymerized by usual radical initiators in spite of their bulky suubstituents[1–5]. Recently we have found that the propagating polymer radicals are stable enough to be ESR-detectable in the radical polymerizations of *N*-substituted maleimides[6,7] and some itaconate esters including bis(2-ethylhexyl) itaconate[8–10], and reported kinetic and ESR results of their radical polymerizations.

Recent attention has been paid to the penultimate effect in the radical copolymerization[11–16]. The results of the copolymerization kinetics by Fukuda et al. revealed that a considerable penultimate effect appears even in the copolymerizations between common comonomers such as methyl methacrylate and styrene[15,16]. The copolymeri-

 CCC 0025-116X/93/$05.00

zation system of *N*-cyclohexylmaleimide (**1**) and bis(2-ethylhexyl) itaconate (**2**) is possible to serve as a powerful tool for elucidating the penultimate effect in the radical copolymerization, because the copolymerization system is expected to also involve ESR-detectable propagating polymer radicals.

The present paper deals with the kinetic and ESR results on the copolymerization of **1** and **2** with the initiator dimethyl 2,2′-azoisobutyrate (**3**) in benzene.

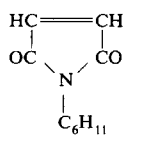

1

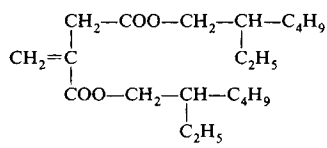

2

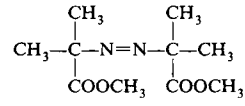

3

Experimental part

N-Cyclohexylmaleimide (**1**) (supplied by Nippon Oil & Fats Co.) was recrystallized from a water-methanol mixture and then once more from methanol. Commercially available bis(2-ethylhexyl)itaconate (**2**) was treated with an aqueous NaOH solution, dried over sodium sulfate and distilled. Dimethyl 2,2′-azoisobutyrate (**3**) was recrystallized from methanol. Benzene was purified by the usual method.

Copolymerization of **1** and **2** with initiator **3** was carried out in a degassed and sealed tube. The resulting copolymer was isolated by pouring the polymerization mixture into a large amount of methanol, dried i. vac. and weighed.

The number-average ($\overline{M}_n$) and weight-average ($\overline{M}_w$) molecular weights of the copolymers were determined by gel permeation chromatography (GPC) using polystyrene standards. GPC was recorded by a TOSO-HLC 802 A at 38 °C, with tetrahydrofuran as the carrier. An ESR spectrum of the copolymerization mixture in a degassed and sealed ESR tube was recorded with a JEOL-JES-FE2XG spectrometer operating at X-band (9,5 GHz) with a TE mode cavity.

Results and discussion

Copolymerization of **1** *and* **2** *with initiator* **3** *in benzene*

Copolymerization of **1** (M_1) and **2** (M_2) with **3** was carried out in benzene at 50 °C. Tab. 1 summarizes the copolymerization results obtained. The composition of the copolymer was determined from the nitrogen content by elemental analysis. Fig. 1 shows the Kelen-Tüdős plot[17] for the copolymerization results. From the plot, the monomer reactivity ratios were obtained as $r_1 = 0{,}34$ and $r_2 = 0{,}38$. As shown in Fig. 2, the observed copolymer compositions show an excellent fit to the composition curve calculated by using the above values of r_1 and r_2.

Fig. 3 shows the time-conversion plots made at 50 °C at various monomer feed compositions, fixing the total monomer concentration of 1,00 mol · L^{-1}. The copolymerization rate (R_p) was estimated using the time-conversion plot and the copolymer composition. Tab. 2 presents the R_p value at each monomer feed composition and the molecular weights of the resulting copolymer. As can be seen from Tab. 2, R_p and $\overline{M}_n$ increase with increasing concentration of **1**.

Tab. 1. Results of copolymerization of **1** (M_1) and **2** (M_2) with initiator **3** at 50 °C in benzene[a)]

Content of M_1 in feed in mol-%	Time in min	Yield in %	Nitrogen content in %	Content of M_1 units in copolymer in mol-%
12,5	70	7,3	1,03	23,1
25,0	40	7,3	1,53	32,5
37,5	40	10,4	2,11	42,2
50,0	25	10,1	2,43	47,1
62,5	20	9,5	3,17	57,4
75,0	15	8,7	3,95	66,9
87,5	10	5,5	4,54	73,2

a) $[M_1] + [M_2] = 1{,}00\ \text{mol} \cdot \text{L}^{-1}$; $[3] = 3{,}00 \cdot 10^{-2}\ \text{mol} \cdot \text{L}^{-1}$.

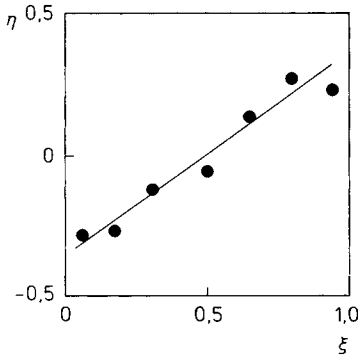

Fig. 1.

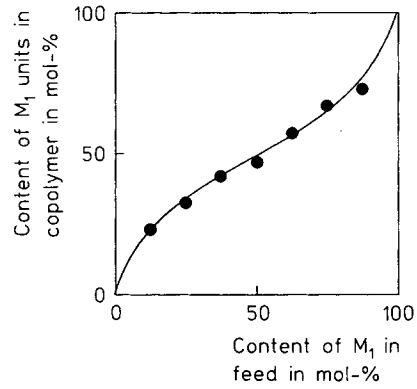

Fig. 2.

Fig. 1. Kelen-Tüdős plot for the copolymerization of **1** (M_1) and **2** (M_2) at 50 °C in benzene

Fig. 2. Copolymer composition curve obtained in the copolymerization of **1** (M_1) and **2** (M_2) at 50 °C in benzene. The circles are observed values, and the solid line is calculated using r_1 = 0,34 and r_2 = 0,38

Fig. 4 shows the relationship between R_p and the concentration of **3** observed at 50 °C, where **[1]** = **[2]** = 0,50 mol · L^{-1}. Thus, R_p is proportional to the square root of initiator concentration, indicating that usual bimolecular termination also occurs in the present copolymerization.

ESR observation of the propagating polymer radicals in the copolymerization system

As mentioned in the introduction, the propagating polymer radicals of **1** and **2** are observable by ESR in the homopolymerization systems. Since termination reactions are diffusion-controlled in the usual radical polymerizations, the propagating polymer

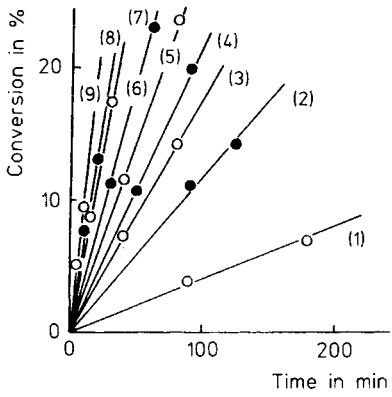

Fig. 3. Time-conversion plots obtained in the copolymerization of **1** and **2** with initiator **3** at 50 °C in benzene. [**3**] = $3{,}00 \cdot 10^{-2}$ mol · L^{-1}, [**1**] + [**2**] = 1,00 mol · L^{-1}. 10 · [**1**] = 0,0 (1), 1,25 (2), 2,50 (3), 3,75 (4), 5,00 (5), 6,25 (6), 7,50 (7), 8,75 (8) and 10,0 (9) mol · L^{-1}

Tab. 2. Copolymerization rate (R_p) and number- and weight-average molecular weights ($\bar{M}_n$ and $\bar{M}_w$) of the copolymers in the copolymerization of **1** and **2** with **3** at 50 °C in benzene[a)]

$10 \cdot$ [**1**] in mol · L^{-1}	$10^6 \cdot R_p$ in mol · $L^{-1} \cdot s^{-1}$	$10^{-4} \cdot \bar{M}_n$	$10^{-4} \cdot \bar{M}_w$	$\bar{M}_w/\bar{M}_n$
0,0	7,16	1,11	1,59	1,4
1,25	18,4	2,56	4,96	1,9
2,50	31,7	2,94	6,08	2,1
3,75	44,4	2,96	5,41	1,8
5,00	54,8	3,60	6,61	1,8
6,25	76,2	4,42	8,23	1,9
7,50	81,7	5,30	10,5	2,0
8,75	114	7,97	16,3	2,1
10,0	204	—	—	—

a) [**1**] + [**2**] = 1,00 mol · L^{-1}; [**3**] = $3{,}00 \cdot 10^{-2}$ mol · L^{-1}.

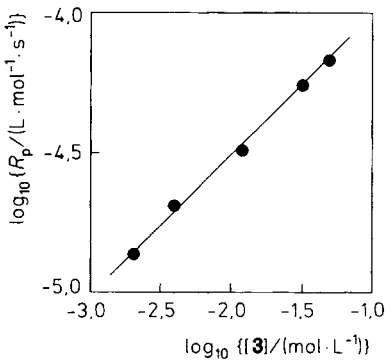

Fig. 4. Relationship between the copolymerization rate (R_p) and the initiator concentration at 50 °C in benzene. [**1**] = [**2**] = 0,50 mol · L^{-1}

radicals are also expected to be ESR-detectable in the copolymerization of **1** and **2**. In fact, as shown in Fig. 5, the copolymerization system was found to involve persistent propagating polymer radicals under the actual polymerization conditions.

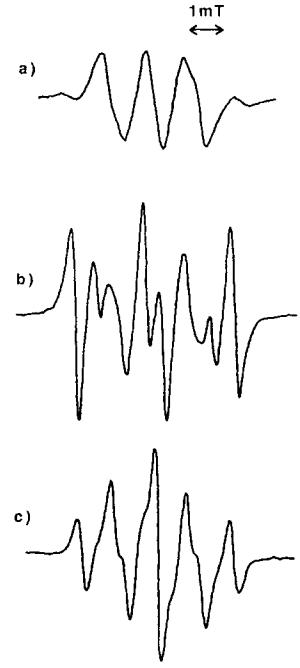

Fig. 5. ESR spectra observed at 50 °C in the systems **1/3** (a), **1/2/3** (b), and **2/3** (c)

Fig. 5 b shows a typical ESR spectrum of the copolymerization system observed at 50 °C at [**1**] = [**2**] = 0,50 mol · L^{-1}. Fig. 5 also compares the ESR spectra of propagating polymer radicals, **4** (spectrum a)) and **5** (spectrum c)), observed in the corresponding homopolymerization systems.

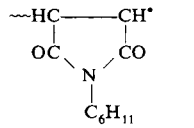

4

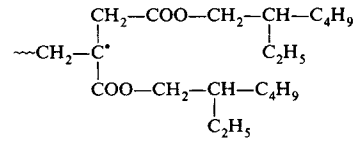

5

As can be seen from Fig. 5, spectrum (b) shows much stronger absorptions at both outer sides compared to spectra (a) and (c), and hence is not explicable in terms of any overlapping of spectra (a) and (c). This reveals that some penultimate monomeric unit causes a change in the ESR spectum, namely, the structure of the propagating radical end.

The total concentration ([$P^{\bullet}$]) of the propagating polymer radicals was determined at 50 °C by computer double integration of the first-derivative ESR spectrum of the copolymerization system, where 2,2,6,6-tetramethylpiperidin-1-oxyl radical (TEMPO), a stable radical, in the same medium was used as reference. Tab. 3 presents the results obtained at various feed monomer compositions. As shown in Fig. 6, the total con-

Tab. 3. Propagating polymer radical concentration ([P•]), apparent rate constants of propagating (k_p) and termination (k_t), and initiator efficiency (f) in the copolymerization of **1** and **2** with **3** at 50 °C in benzene[a)]

$10 \cdot$ [1] in mol · L^{-1}	$10^6 \cdot$ [P•] in mol · L^{-1}	k_p in L · mol^{-1} · s^{-1}	f	$10^{-3} \cdot k_t$ in L · mol^{-1} · s^{-1}
0,0	4,7	1,5	0,49	3,0
1,25	4,8	3,8	0,49	2,8
2,50	5,0	6,3	0,49	2,6
3,75	6,4	6,9	0,64	2,1
5,00	6,8	8,1	0,68	2,0
6,25	7,0	10,9	0,68	1,8
7,50	6,6	12,4	0,68	2,1
8,75	6,0	18,9	0,68	2,5
10,0	4,1	50,1	0,68	5,4

a) [1] + [2] = 1,00 mol · L^{-1}; [3] = 3,00 · 10^{-2} mol · L^{-1}.

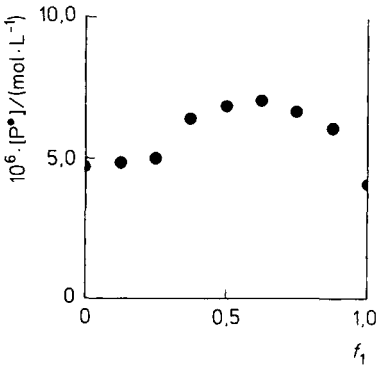

Fig. 6. Relationship between the propagating polymer radical concentration ([P•]) and the monomer feed composition (f_1 = [1]/([1] + [2]))

centration of propagating polymer radicals shows a flat maximum on varying the monomer feed composition.

Determination of the apparent rate constant of propagation in the copolymerization

Using R_p (Tab. 2) and the total concentration ([P•]) of propagating polymer radicals (Tab. 3), the apparent rate constant (k_p) of propagation in the copolymerization at 50 °C was determined according to Eq. (1), where [M] = [1] + [2] = 1,00 mol · L^{-1}.

$$R_p = k_p \cdot [P^\bullet][M] \quad (1)$$

The k_p values thus obtained are also summarized in Tab. 3. The apparent rate constant for the copolymerization increases with increasing concentration of **1**. Fig. 7 shows the relationship between k_p and the monomer feed composition (f_1 = [1]/([1] + [2])).

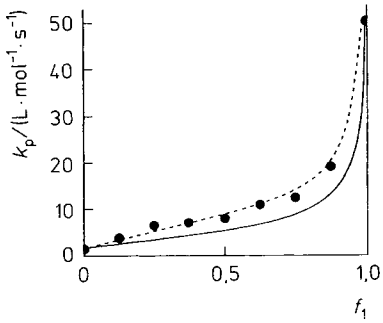

Fig. 7. Relationship between the apparent rate constant of propagation (k_p) and the monomer feed composition (f_1 = [1]/([1] + [2])). The circles are observed values, and the solid and dashed lines represent the Mayo-Lewis and penultimate (s_1 = 0,15; s_2 = 3,4) model predictions, respectively

On the other hand, the apparent prapagation rate constant of copolymerization is calculated using Eq. (2) based on the Mayo-Lewis model, where k_{11} is the propagation rate constant of M_1 (**1**) and k_{22} the propagation rate constant of M_2 (**2**), and $f_2 = (1 - f_1)$.

$$k_p = (r_1 \cdot f_1 + 2f_1 \cdot f_2 + r_2 \cdot f_2)/(r_1 \cdot f_1/k_{11} + r_2 \cdot f_2/k_{22}) \quad (2)$$

The calculated k_p values are also plotted against f_1 in Fig. 7. Thus, the observed k_p values are fairly higher than the calculated ones. Such deviations are attributable to the penultimate effect.

A model to describe the experimental data was proposed by Fukuda et al. [15,16]. The model says that the ordinary monomer reactivity ratios, r_1 and r_2, are not affected by the penultimate unit, but the ratios $s_1 = k_{211}/k_{111}$ and $s_2 = k_{122}/k_{222}$ differ from unity because of the penultimate effect (Eqs. (5)–(12)). With these assumptions, the k_{11} and k_{22} terms in Eq. (2) are as follows:

$$k_{11} = k_{111} \cdot (r_1 \cdot f_1 + f_2)/(r_1 \cdot f_1 + f_2/s_1) \quad (3)$$

$$k_{22} = k_{222} \cdot (r_2 \cdot f_2 + f_1)/(r_2 \cdot f_2 + f_1/s_2) \quad (4)$$

Since the observed copolymer composition agrees closely with the composition curve calculated using r_1 = 0,34 and r_2 = 0,38 as shown in Fig. 2, Fukuda's model is applicable to the present copolymerization.

We have attempted to determine the values of s_1 and s_2 so that the observed apparent k_p values in Fig. 7 show the best fit to the relation derived by substituting Eqs. (3) and (4) in Eq. (2) on the basis of the nonlinear least-squares method. The following values were obtained:

$$s_1 = 0{,}15 \qquad s_2 = 3{,}4$$

Using these figures the apparent k_p values were calculated and are shown as a dashed line in Fig. 7.

Using the above findings, the following rate constants of eight propagations for the penultimate model were estimated for the copolymerization of **1** (M_1) and **2** (M_2) at 50 °C in benzene.

$$R-M_1M_1^{\bullet} + M_1 \xrightarrow{k_{111} = 50\ L \cdot mol^{-1} \cdot s^{-1}} R-M_1M_1M_1^{\bullet} \quad (5)$$

$$R-M_2M_1^{\bullet} + M_1 \xrightarrow{k_{211} = 7{,}5\ L \cdot mol^{-1} \cdot s^{-1}} R-M_2M_1M_1^{\bullet} \quad (6)$$

$$R-M_1M_1^{\bullet} + M_2 \xrightarrow{k_{112} = 147\ L \cdot mol^{-1} \cdot s^{-1}} R-M_1M_1M_2^{\bullet} \quad (7)$$

$$R-M_2M_1^{\bullet} + M_2 \xrightarrow{k_{212} = 22\ L \cdot mol^{-1} \cdot s^{-1}} R-M_2M_1M_2^{\bullet} \quad (8)$$

$$R-M_2M_2^{\bullet} + M_1 \xrightarrow{k_{221} = 3{,}9\ L \cdot mol^{-1} \cdot s^{-1}} R-M_2M_2M_1^{\bullet} \quad (9)$$

$$R-M_1M_2^{\bullet} + M_1 \xrightarrow{k_{121} = 13\ L \cdot mol^{-1} \cdot s^{-1}} R-M_1M_2M_1^{\bullet} \quad (10)$$

$$R-M_2M_2^{\bullet} + M_2 \xrightarrow{k_{222} = 1{,}5\ L \cdot mol^{-1} \cdot s^{-1}} R-M_2M_2M_2^{\bullet} \quad (11)$$

$$R-M_1M_2^{\bullet} + M_2 \xrightarrow{k_{122} = 5{,}1\ L \cdot mol^{-1} \cdot s^{-1}} R-M_1M_2M_2^{\bullet} \quad (12)$$

Such a large suppression in reactivity of the **1** radical by a penultimate monomeric unit **2** results probably from the steric hindrance due to the bulky 2-ethylhexyl groups of **2**. In contrast, the reactivity of the **2** radical is 3,5 times enhanced by a penultimate monomeric unit **1**. This comes probably from a release of the steric strain in the successive monomeric unit **2** linkages.

Determination of the apparent rate constant of termination in the copolymerization

To evaluate the apparent rate constant of termination (k_t), we have determined the initiator efficiency (f) of **3** in the present copolymerization system at 50 °C in the same manner as described in a previous paper[6], where **3** was allowed to decompose in the copolymerization system containing a small amount of TEMPO.

3 decomposes into 1-methoxycarbonyl-1-methylethyl radical and nitrogen:

$$3 \longrightarrow 2\ CH_3-\overset{CH_3}{\underset{COOCH_3}{\overset{|}{\underset{|}{C^{\bullet}}}}} + N_2 \quad (13)$$

Some of the primary radicals are deactivated by the cage reactions. The others diffuse through the solvent cage to be trapped by TEMPO. So, the f values could be estimated from the disappearance rate of TEMPO by ESR, where the rate constant of $k_d = 2{,}22 \cdot 10^{-6}\ s^{-1}$ was used for the decomposition of **3** at 50 °C[18]. The results obtained at various monomer feed compositions are also presented in Tab. 3. The f value shows a tendency to decrease with increasing concentration of **2**, which is due to the high viscosity of **2**.

Using the concentration ([P•]) of propagating polymer radicals and the f value, k_t was determined at each monomer feed composition according to Eq. (6).

$$2k_d \cdot [3] = k_t \cdot [P^\bullet]^2 \tag{6}$$

Tab. 3 also summarizes the results obtained.

Fig. 8 shows the relationship between the k_t value and the monomer feed composition. Thus, k_t shows a flat minimum on changing the monomer feed composition. Since the termination reactions are diffusion-controlled in the radical polymerizations, the k_t value might reflect the structure of propagating polymer radicals in the copolymerization system. So, the intrinsic viscosity ([η]) of the copolymer formed at each monomer feed composition was measured at 30 °C in benzene by an Ubbelohde viscosimeter and is shown in Fig. 9. Thus [η] is found to exhibit a behaviour similar to the k_t value. This indicates that the more compactly coiled propagating polymer radical shows a smaller k_t value in the present copolymerization system.

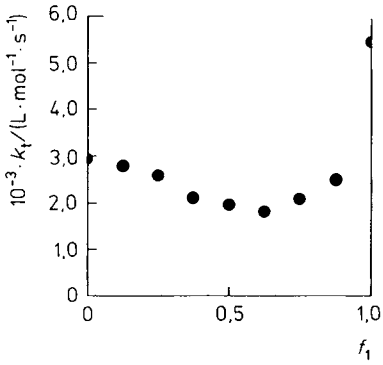

Fig. 8.

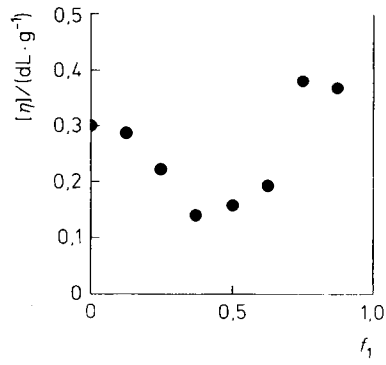

Fig. 9

Fig. 8. Relationship between the apparent rate constant of termination (k_t) and the monomer feed composition (f_1 = [1]/([1] + [2]))

Fig. 9. Relationship between the intrinsic viscosity ([η]) of copolymer and the monomer feed composition (f_1 = [1]/([1] + [2]))

[1] S. Nagai, K. Yoshida, *Kobunshi Kagaku* **17**, 791 (1960)
[2] M. G. Baldwin, S. F. Keed, *J. Polym. Sci., Part A:* **1**, 79 (1963)
[3] T. Oishi, T. Kimura, *Kobunshi Ronbunshu* **33**, 685 (1976)
[4] J. M. Barrales-Rienda, J. M. Mazón-Arecherra, *Macromolecules* **20**, 1637 (1987)
[5] A. Matsumoto, Y. Oki, T. Otsu, *Polym. J. (Tokyo)* **23**, 201 (1991)
[6] T. Sato, K. Arimoto, H. Tanaka, T. Ota, K. Kato, K. Doiuchi, *Macromolecules* **22**, 2219 (1989)
[7] T. Sato, K. Masaki, M. Seno, H. Tanaka, *Makromol. Chem.* **194**, 849 (1993)
[8] T. Sato, S. Inui, H. Tanaka, T. Ota, M. Kamachi, K. Tanaka, *J. Polym. Sci., Part A: Polym. Chem.* **25**, 637 (1987)
[9] T. Sato, K. Morino, H. Tanaka, T. Ota, *Makromol. Chem.* **188**, 2951 (1987)
[10] T. Sato, Y. Takahashi, M. Seno, H. Nakamura, H. Tanaka, *Makromol. Chem.* **192**, 2909 (1991)
[11] S. A. Jones, G. S. Prementine, D. A. Tirrell, *J. Am. Chem. Soc.* **107**, 5275 (1985)

[12] T. Kelen, F. Tüdős, D. Braun, W. K. Czerwinski, *Makromol. Chem.* **191**, 1853 (1990)
[13] M. C. Piton, M. A. Winnik, T. P. Davis, K. F. O'Driscoll, *J. Polym. Sci.: Part A: Polym. Chem.* **28**, 2097 (1990)
[14] T. P. Davis, K. F. O'Driscoll, M. C. Piton, M. A. Winnik, *Macromolecules* **23**, 2113 (1990)
[15] T. Fukuda, Y.-D. Ma, H. Inagaki, *Makromol. Chem., Suppl.* **12**, 125 (1985)
[16] T. Fukuda, Y.-D. Ma, H. Inagaki, *Macromolecules* **18**, 17 (1985)
[17] T. Kelen, T. Tüdős, *J. Macromol. Sci. Chem.* **A16**, 1283 (1981)
[18] T. Otsu, B. Yamada, *J. Macromol. Sci. Chem.* **A3**, 187 (1969)